A Hydrogen Storage Mechanism in Single-Walled Carbon Nanotubes

Seung Mi Lee,[†,‡,⊥] Kay Hyeok An,[‡] Young Hee Lee,*[,†,‡,§] Gotthard Seifert,[∥] and Thomas Frauenheim[∥]

Contribution from the Department of Semiconductor Science and Technology, Semiconductor Physics Research Center, and Department of Physics, Jeonbuk National University, Jeonju 561-756, R. O. Korea, and Universität-GH Paderborn, Fachbereich Physik, Theoretische Physik, 33095 Paderborn, Germany

Abstract: We have carried out systematic calculations for hydrogen-adsorption and -storage mechanism in carbon nanotubes at zero temperature. Hydrogen atoms first adsorb on the tube wall in an *arch*-type and *zigzag*-type up to a coverage of $\theta = 1.0$ and are stored in the capillary as a form of H_2 molecule at higher coverages. Hydrogen atoms can be stored dominantly through the tube wall by breaking the C−C midbond, while preserving the wall stability of a nanotube after complete hydrogen insertion, rather than by the capillarity effect through the ends of nanotubes. In the hydrogen-extraction processes, H_2 molecule in the capillary of nanotubes first dissociates and adsorbs onto the inner wall and is further extracted to the outer wall by the flip-out mechanism. Our calculations describe suitably an electrochemical storage process of hydrogen, which is applicable for the secondary hydrogen battery.

I. Introduction

Despite tremendous efforts to use hydrogen as a source of energy, developing a stable storage vehicle of a large amount of hydrogens has never been easily accessible.[1] It is always desirable to develop a new storage vehicle with high capacity, light mass, and high stability, which may be applicable for portable electronics and moving vehicles. The carbon nanotubes (CNTs) seem to be an ultimate material for this, due to their chemical stability, large surface area, hollowness, and light mass.[2] Hydrogen could be stored in bundles of single-walled nanotubes, where H_2 molecules are physisorbed at the exterior surfaces of CNTs or interstitial spaces between CNTs separating the intertube distances, under high pressure of hydrogen gas.[3−5] The storage capacity was reported to be about 8 wt % under 77 K,[3] while that under room temperature varied as reported by research groups.[4,5] These high values of hydrogen storage under room temperature are still doubtful in the society. Early Monte Carlo simulations predicted about 1 wt % at 10 MPa,[6] whereas some recent calculations predicted large values up to 10−14 wt % at low temperature.[7−9] Another molecular dynamics simulation predicts that carbon nanotubes are not suitable sorbent material for achieving DOE targets of hydrogen storage.[10] Thus there still disagreements between experiments and theoretical predictions, which are highly debatable at this moment.

It has also been demonstrated that CNTs could also store hydrogens electrochemically at less than 1 wt %,[11,12] yet far from the useful amount of 6.5 wt %, which is required by the DOE hydrogen plan,[13] even though the electrochemical method is more practical for the application to the secondary hydrogen battery. In the latter case, it is not the hydrogen molecules but the hydrogen ions (or hydrated hydrogen ions) that exist in an electrolyte, leading to a different adsorption mechanism from the previously described physisorption process, where the H_2 molecule plays an important role for adsorption. An efficient method of hydrogen storage, maximum storage capacity, a form of hydrogen adsorption, and reversibility, especially in an electrochemical storage method, are still far from being clearly understood. The theoretical model calculations can show the hydrogen adsorption and storage mechanism in atomic scale. It is our intention to describe the chemisorption and storage mechanism which can interpret an electrochemical process. Note that the density-functional calculations we adopt in this paper are valid at zero temperature. Furthermore, understanding the adsorption mechanism is a key ingredient to predict the maximum storage capacity and to provide a road map for the development of the CNT-based hydrogen storage vehicle.

II. Calculation Methods

For our calculations we use a self-consistent charge density-functional-based tight-binding method (SCC-DFTB). The SCC-DFTB method uses a basis of numerically described s and p atomic orbitals

* To whom correspondence should be addressed. Present address: Department of Physics, Sungkyunkwan University, Suwon 440-746, Korea. E-mail: leeyoung@yurim.skku.ac.kr.

† Department of Semiconductor Science and Technology, Jeonbuk National University.

‡ Semiconductor Physics Research Center, Jeonbuk National University.

§ Department of Physics, Jeonbuk National University.

∥ Universität-GH Paderborn.

⊥ Present address: Fritz-Haber-Institut der MPG, Faradayweg 4-6, D-14195, Berlin, Germany.

(1) Dresselhaus, M. S.; Williams, K. A.; Eklund, P. C. *MRS Bull.* **1999**, *24*, 45−50 and references therein.

(2) The specific area of CNTs are known as smaller than that of activated carbon.

(3) Ye, Y.; Ahn, C. C.; Witham, C.; Fultz, B.; Liu, J.; Rinzler, A. G.; Colbert, D.; Smith, K. A.; Smalley, R. E. *Appl. Phys. Lett.* **1999**, *74*, 2307−2309.

(4) Dillon, A. C.; Jones, K. M.; Bekkedahl, T. A.; Kiang, C. H.; Bethune, D. S.; Heben, M. J. *Nature* **1997**, *386*, 377−379.

(5) Liu, C.; Fan, Y. Y.; Liu, M.; Cong, H. T.; Cheng, H. M.; Dresselhaus, M. S. *Science* **1999**, *286*, 1127−1129.

(6) Rzepka, M.; Lamp, P.; de la Casa-Lillo, M. A. *J. Phys. Chem.* **1998**, *102*, 10894−10898.

(7) Darkrim, F.; Levesque, D. *J. Phys. Chem. B* **2000**, *104*, 6773−6776.

(8) Williams, K. A.; Eklund, P. C. *Chem. Phys. Lett.* **2000**, *320*, 352−358.

(9) Lee, S. M.; Lee, Y. H. *Appl. Phys. Lett.* **2000**, *76*, 2877−2879.

(10) Wang, Q.; Johnson, J. K. *J. Chem. Phys.* **1999**, *100*, 577−586.

(11) Nutzenadel, C.; Zuttel, A.; Chartouni, D.; Schlapbach, L. *Electrochem. Solid−State Lett.* **1999**, *2*, 30−32.

(12) Lee, S. M.; Park, K. S.; Choi, Y. C.; Park, Y. S.; Bok, J. M.; Bae, D. J.; Nahm, K. S.; Choi, Y. G.; Yu, S. C.; Kim, N.; Frauenheim, T.; Lee, Y. H. *Synth. Met.* **2000**, *113*, 209−216.

(13) DeLuchi, M. *Hydrogen Fuel-Cell Vehicles*; Institute of Transportation Studies, University California: Davis, 1992.

10.1021/ja003751+ CCC: $20.00
Published on Web 05/05/2001

for carbon and s orbital for hydrogen. Hamiltonian and overlap matrix elements are evaluated by a two-center approach. Charge transfer is taken into account through the incorporation of a self-consistency scheme for Mulliken charges on the basis of the second-order expansion of the Kohn−Sham energy in terms of charge density fluctuations. The diagonal elements of the Hamiltonian matrix employed are then modified by the charge-dependent contributions to describe the change in the atomic potentials due to the charge transfer. The off-diagonal elements have additional charge-dependent terms due to the Coulombic potential of ions. They decay as $1/r$ and thus account for the Madelung energy of the system. Further details of the SCC-DFTB method have been published elsewhere.[14]

Although the SCC-DFTB approaches are very efficient to describe the systems quantum mechanically, the accuracy test is demanding in some cases. To check the validity of SCC-DFTB approach, we also perform state of the art technique, the DF total energy calculations based on the local density approximation (LDA) and generalized gradient approximation (GGA).[15] The exchange-correlation energy in LDA is parametrized by Perdew and Wang's scheme,[16] and Becke's corrected exchange functional[17] is adopted in GGA calculations. All-electron Kohn−Sham wave functions are expanded in a local atomic orbital basis. All orbitals including core electrons, are taken into account throughout the calculations. In the double-numerical basis set, C-2s and C-2p orbitals are represented by two basis functions each, and a 3d-type wave function for carbon atom is used to describe polarization. The convergency criterion for the structure optimization is that all forces be ≤ 0.001 au, and the energy change for the charge density per self-iteration be $\leq 1.0 \times 10^{-5}$ Ha. Structure optimization is done by the SCC-DFTB and LDA schemes. The GGA calculations are done with structures optimized by LDA whenever necessary. It is worth noting that the calculations are valid at zero temperature.

III. Results and Discussion

A. Adsorption Geometry. We now choose a supercell of (5,5) armchair nanotube in our calculations for the sake of simplicity. The periodic boundary condition is applied along the tube axis. The diameter of the (5,5) nanotube after full relaxation of the geometry by the conjugate gradient method is 6.88 Å, similar to that of C_{60}, with the average C−C bond lengths of 1.44 Å, as shown in Figure 1a. In the electrochemical process of hydrogen adsorption, the ambient species of hydrogens in an electrolyte are hydrogen ions. These will exothermally adsorb at the top sites of carbon atoms on the tube wall, forming an *arch*-type, as shown in Figure 1b. Hydrogens with up to a coverage $\theta = 1.0$ or equivalently 7.7 Hwt % can be stored in an *arch*-type tube. This enhances sp^3-like hybridizations in the tube and expands the CNT diameter to 7.78 Å. The average C−C bond lengths are enlarged to 1.54 Å, still maintaining strong covalent bonds, similar to those of a diamond. The C−H bond length is 1.12 Å, similar to 1.1 Å of CH_4 molecule. Geometries optimized with the LDA were not much different from those optimized with the SCC-DFTB. The binding energy[18] of the C−H bond is −2.65 eV per C−H bond,[19] about half the C−H covalent bond energy of CH_4 molecule. We find another stable geometry, a *zigzag*-type, where hydrogen atoms are bound alternatively at the exterior and interior of the CNT, as shown in Figure 1c. This geometry is more stable than the *arch*-type by 0.56 eV per C−H bond. The structure is stabilized by minimizing strains of the C−C bonds, resulting in less expansion of the average diameter (7.13 Å). This leads to the C−C and C−H bond angles of 103° and 108°, representing more severe sp^3 hybridizations than the *arch*-type. Figure 1d represents another stable geometry, where molecular hydrogens are stored in an empty space inside the CNT. The binding energy of a H_2 molecule is −4.57 eV, still covalent bonding but weaker than that of a gaseous molecule by 1.96 eV. The weak binding energies of molecular hydrogens inside the nanotube originate from the repulsive energies between H_2 molecules and those between H_2 molecules and the tube wall.[9] Thus, the diameter is expanded by 8%, similar to the lattice expansion of the *c*-axis in the graphite during the hydrogen intercalation. The repulsive forces due to the antibonding states also determine the maximum storage capacity. Therefore, we expect the CNTs with larger diameter to increase the storage capacity. In fact, the storage capacity of hydrogen in an empty space increases linearly with the tube diameter.[9]

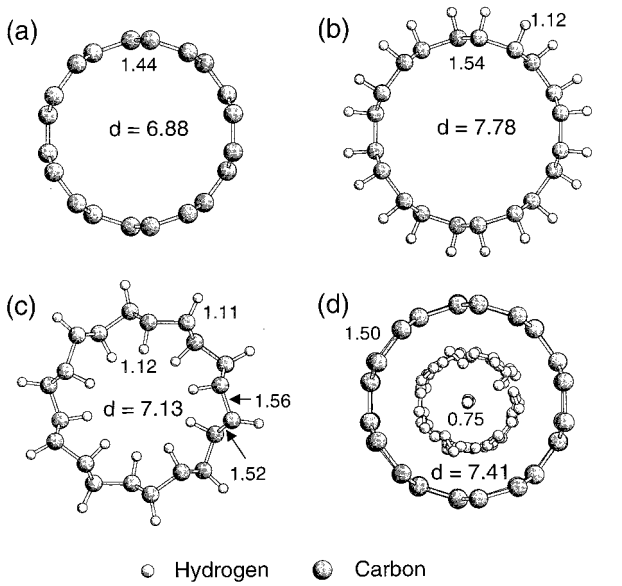

Figure 1. Top views of various hydrogen adsorptions in the (5,5) nanotube with ball-and-stick forms; (a) clean, (b) *arch*-type, (c) *zigzag*-type, and (d) the molecular hydrogens inside the CNT with $\theta \geq 1.0$. The *d* indicates an average diameter of the CNT. Bond lengths are in units of Å.

B. Storage Mechanism. Although the *zigzag*-type or H_2 molecules in the capillary is energetically more stable than the *arch*-type, it is not clear how the hydrogen atoms can be inserted into the capillary of nanotubes. One may imagine a simple capillarity effect, where hydrogens can be inserted through the open ends.[4,20,21] Since the aspect ratio of the CNT is usually up to $10^4 \sim 10^6$, it is very unlikely that hydrogens inside the CNTs are accommodated exclusively by the capillarity effect through the open-ends. This suggests a new possibility of the hydrogen-storage mechanism into the CNTs. Here we introduce several H-insertion mechanisms through the tube wall. We have searched for a reaction pathway which gives rise to a relatively low activation barrier for a hydrogen atom to penetrate through the wall. Furthermore, the CNTs should not be fragmented during the hydrogen storage process. An inappropriately chosen pathway will result in a large activation barrier and disintegrate the CNT wall in some cases. Therefore, our reaction pathways will provide an upper bound of the realistic activation barrier.

(14) Elstner, M.; Porezag, D.; Jungnickel, G.; Elsner, J.; Haugk, M.; Frauenheim, T.; Suhai, S.; Geifert, G. *Phys. Rev. B* **1998**, *58*, 7260−7268.

(15) DMol3 is a registered software product of Molecular Simulations Inc.

(16) Perdew, J. P.; Wang, Y. *Phys. Rev. B.* **1992**, *45*, 13244−13249.

(17) Becke, A. D. J. *Chem. Phys.* **1988**, *88*, 2547−2553.

(18) The binding energy of C−H bond is calculated by, $E_b(\text{C−H}) = E_{total}(\text{CNT} + \text{H}) - E_{total}(\text{CNT}) - N_H E_{atom}(\text{H})$.

(19) The binding energy is overestimated by 0.9 eV in the SCC-DFTB, compared to the GGA calculations. However, the energy differences for different configurations were small.

(20) Pederson, M. R.; Broughton, J. Q. *Phys. Rev. Lett.* **1992**, *69*, 2689−2692.

(21) Ajayan, P. M.; Iijima, S. *Nature* **1993**, *361*, 333−334.

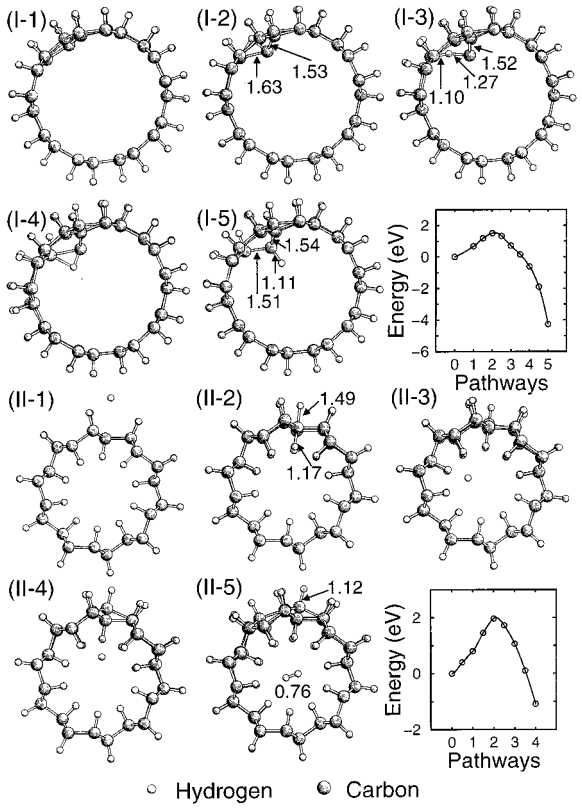

Figure 2. Concerted reaction pathways and the corresponding potential barriers for hydrogen insertion of (I) flip-in and (II) kick-in mechanism. Bond lengths are in units of Å. Reaction coordinate "0" indicates the corresponding reference (I: *arch*-type, II: *zigzag*-type).

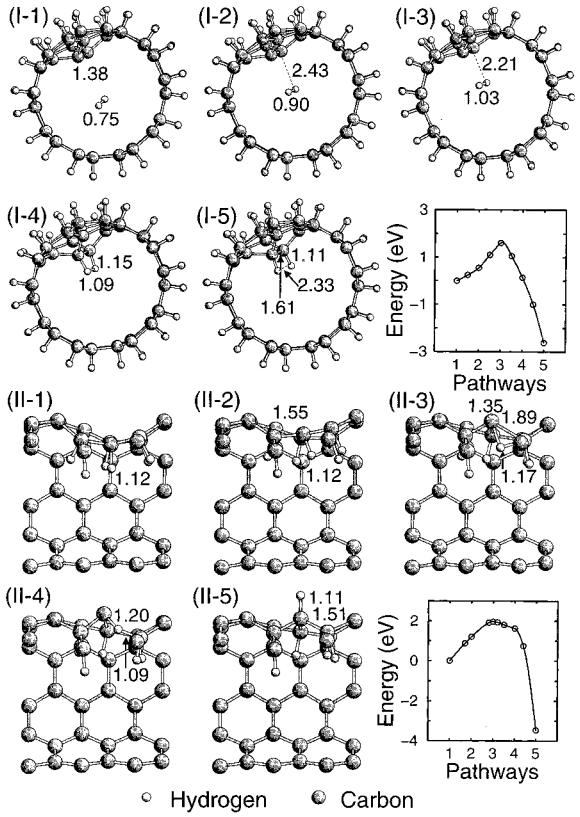

Figure 3. Concerted reaction pathways and the corresponding potential barriers for (I) readsorption of molecular hydrogen in the capillary to the interior of the tube wall and (II) flip-out process. Bond lengths are in units of Å.

We first consider a flip-in mechanism, as shown in Figure 2(I). The hydrogen atom located at the top site of the *arch*-type pushes down the carbon atom and then flips into the C−C midbond.[22,23] The activation barrier of 1.51 eV appears in the step (I-2). The sp^3 bonds are still maintained locally in the step (I-2), resulting in reasonably small activation barrier. Most energy costs result from the bond-stretchings of the carbon atom (1.53, 1.63 Å) attached to the hydrogen atom. The C−C midbond is broken during the flip-in process. After the hydrogen atom is flipped into the capillary, the C−C bond is recovered exothermally, ensuring the CNT stability, as shown in the step (I-4). Full relaxation of the hydrogen atom finally minimizes the strain energies between carbon atoms and bond-angle distortions, as shown in the step (I-5), reaching the stable inner top site. It is worth noting that the flip-in process works by maintaining the CNT walls stable only at coverage $\theta = 1.0$. In cases of a hydrogen coverage of $\theta < 1.0$, the heavy strain is involved in the flip-in process, which gives rise to a large activation barrier of ≥ 3.5 eV and breaks the tube wall.[24] The C−C bond weakening (1.54 Å from 1.44 Å) by the hydrogenation (still forming strong covalent bonds) plays a crucial role in lowering the activation barrier. This suggests a stepwise storage mechanism in which the flip-in process takes place only after the top sites at the exterior of the CNT are fully saturated by the hydrogen atoms.

Hydrogen atom in the next neighboring top site can flip in more easily with an activation barrier of 0.74 eV, leading to a continuous flip-in process. This is expected, since the hydrogen atom at the inner top site reduces the strain energy required to push the next neighboring hydrogen atom toward the carbon atom. Continuing this process reduces severely the diameter of the CNT, making the H−H distance closer, eventually forming molecular hydrogens inside the capillary.[25] One may also consider a *zigzag* flip-in process, that is, a continuous flip-in process in the second-nearest neighbor top site. An activation barrier of 0.93 eV is required, when another hydrogen atom at the top site is pushed toward the carbon atoms.[24] This process will finally result in the *zigzag*-type. The energy barriers and energy gains of both flip-in processes are similar to each other, suggesting that both processes are equally likely to occur.

Once the *zigzag*-type with a coverage $\theta = 1.0$, is formed via a zigzag flip-in process, a mechanism for storing more hydrogens in the capillary for $\theta > 1.0$ is not intuitively clear. We propose here a kick-in mechanism, as shown in pathway II in Figure 2, where a hydrogen atom approaches an empty top site that is occupied by another hydrogen atom in the interior of the tube. Moving a hydrogen atom close to the top site from the outer surface leads to two weak C−H bonds (1.49 and 1.17 Å), as shown in the step (II-2), giving an activation barrier of 1.97 eV. Moving closer to the tube until the C−H bond length becomes 1.0 Å kicks off the hydrogen atom attached in the interior of the tube wall to the capillary. Full relaxation after

(22) We move a hydrogen atom towards the tube wall in each step and then fix the radial component of the hydrogen atom, while relaxing all other carbon atoms in the tube. This relaxation scheme is applied to the rest of the calculations, unless specified.

(23) We have also tried several flip-in processes, where the hydrogen atom rotates through the hexagonal ring. However, rotation of the hydrogen atom to near the graphitic plane induces severe distortions of sp^3 bonds, resulting in the formation of a new CH_2 at the adjacent carbon site and the bond-breaking of the C−C bond. This gives rise to a large activation barrier ≥ 3 eV and furthermore disintegrates the tube wall.

(24) Lee, S. M.; Lee, Y. H. Manuscript in preparation.

(25) The filp-in energy barrier could be modified as the hydrogen density inside the capillary increases.

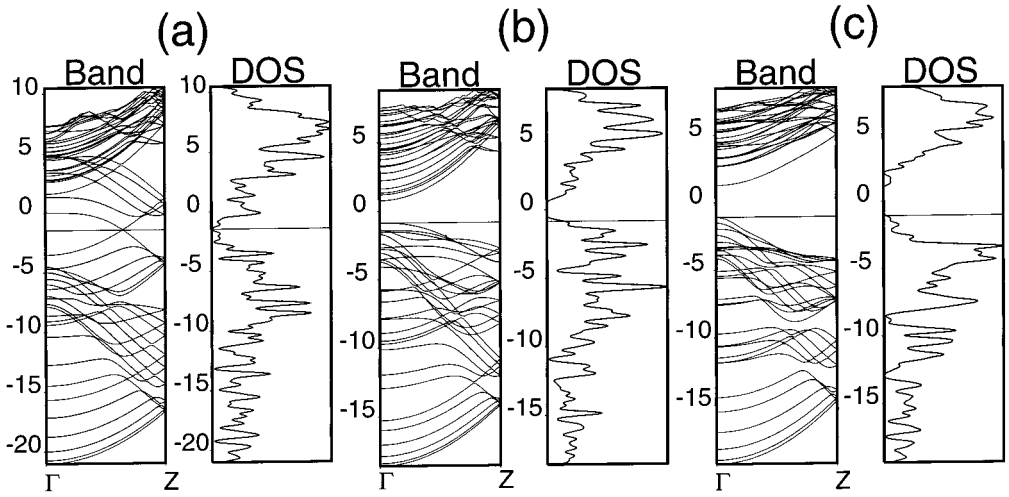

Figure 4. Band dispersions along the tube axis *Z* (0,0, π/2) and the corresponding densities of states for (a) clean (5,5) nanotube, (b) *arch*-type, and (c) *zigzag*-type. The horizontal lines indicate the Fermi level. The energies are in unit of eV.

the kick-in recovers the tube wall to form locally an *arch*-type, as shown in the step (II-4). Repeating the kick-in processes will eventually lead to the formation of molecular hydrogens in the capillary, as shown in the step (II-5), and thus a large storage capacity is expected, similar to that in the continuous flip-in process. Furthermore, the tube wall recovers an *arch*-type and will repeat the whole process discussed above, storing more hydrogens in the capillary until saturated. This may give the maximum hydrogen storage capacity. Considering the most routinely synthesized nanotube of (10,10), the theoretically estimated storage capacity could be as high as 14 Hwt %.[9,26]

C. Extraction Mechanism. To complete the storage mechanism with complete reversibility, we here consider the hydrogen-extraction mechanism. The first question is how the molecular hydrogen in the capillary can be extracted out via the tube wall. The activation barrier should be less than 2.0 eV, and furthermore the tube wall should not be disintegrated during the extraction process. The extraction process is composed of two steps: (i) adsorption of hydrogens in the interior of the tube wall from the molecular hydrogen in the capillary and (ii) the flip-out process, where the hydrogen atom flips out via the tube wall. Molecular hydrogens will not be adsorbed onto the inner wall surface unless some hydrogen atoms are desorbed at the exterior of the tube wall.[27] The inner C−C bond is double-bonded with a bond length of 1.38 Å, as shown in the step (I-1) in Figure 3. Molecular hydrogen will first adsorb onto the exposed bonds of the inner tube wall. As the molecular hydrogen approaches to the double-bonded carbon atoms,[28] the H−H bond length is increased. The barrier of 1.61 eV is reached in the step (I-3). After the step (I-3), the H_2 bond is broken, and instead two C−H bonds are formed exothermally. The inner C−C bond is changed to a single bond, similar to the hydrogenation of an ethylene molecule.

We next consider the second step of the hydrogen-extraction process. The flip-out process, a direct reverse process of the flip-in mechanism from the step (I-5) of Figure 3, can be excluded, since the final structure after the flip-out process will be the step (I-5) in Figure 2, which has higher energy by 4 eV more than that of the starting configuration. One can presumably imagine that the hydrogen atoms at the exterior of the CNT surface are desorbed first and at the same time molecular hydrogens will be adsorbed on those sites during the discharging process, resulting in several hydrogen adsorptions in the interior of the tube wall, as shown in the step (II-1). We test another flip-out mechanism, where one hydrogen atom surrounded by the adjacent hydrogen atoms breaks into the C−C midbond and flips out to the exterior of the tube wall, similar to the reverse flip-in mechanism. In this case, we fixed the position of the chosen hydrogen atom. The barrier exists in the step (II-3) with a barrier height of 1.96 eV. Once the hydrogen atom is moved out of the tube wall, the hydrogen atom takes the top site exothermally, completing the flip-out process, as shown in the step (II-5). Thus, the strong local strain induced by the adsorbed hydrogens in the interior of the tube wall lowered the activation barrier for the flip-out process dramatically. In summary, we show that there are energetically reasonable pathways for a reversible electrochemical storage of hydrogen in CNTs. A crucial role in this storage process plays stable intermediate configurations (the *arch*-type and the *zigzag*-type) and "flipping processes" of the bonded hydrogen through the nanotube wall.

D. Electronic Structures. Finally, it is interesting to see the influence of the C−H bond formation in the nanotubes to the band gap. The pure armchair nanotube shows a metallic behavior, that is, the band-crossing at the Fermi level as shown in Figure 4a.[29] In the *arch* and *zigzag*-type, we see clearly the band-gap opening of 1.63 and 2.63 eV, respectively, due to the sp hybridization, as shown in Figure 4b,c. Since the LDA is known to underestimate the band gap, we expect the gap-openings to be more serious. The present calculations imply several important consequences. The CNT electrode becomes insulating with increasing hydrogen coverage during electrochemical storage process, although the initial CNTs are metallic. A sudden current drop during the discharging process may be observed.[24] Doping or an addition of conductive materials for the CNT electrode is necessary to avoid such a current drop. This should be validated by the experiments.

(26) The calculations in ref 9 are valid only at zero temperature. The extrapolation of the Monte Carlo simulations ref 8 to the zero temperature also gives similar values compared with our results. At liquid nitrogen temperature and some reasonably achievable pressure, this value will be reduced to 5∼10 Hwt %.

(27) Once discharging takes place in experiment, some of hydrogen atoms adsorbed at the exterior of the tube wall can be easily desorbed, resulting in local rearrangement of carbon atoms, as shown in the step (I-1) of Figure 3.

(28) We move H_2 close to the dangling bonds and at the same time H_2 bonds are moved apart. The full relaxation was then done while fixing the positions of H_2.

(29) Planewave basis set with a kinetic energy cutoff of 40 Ry was used in LDA calculations.

IV. Conclusions

We have investigated the hydrogen-adsorption and -storage mechanism in the single-walled carbon nanotubes with density-functional calculations which valid at zero temperature. Several key intermediate states of hydrogen adsorption are identified. Hydrogen atoms can be stored in the capillary through the tube wall by filp-in and kick-in mechanisms, while preserving the wall stability of a nanotube. The H_2 molecule in the capillary of nanotubes first dissociates and adsorbs onto the inner wall, and is further extracted to the outer wall by the flip-out mechanism. Our calculations may describe an electrochemical storage process of hydrogen, which is applicable for the secondary hydrogen battery.

Acknowledgment. This work was supported by the MOST through National Research Laboratory program and in part by KOSEF and in part by the BK21-2001 program.

JA003751+